Hindawi
International Journal of RF and Microwave Computer-Aided Engineering
Volume 2023, Article ID 4034241, 10 pages
https://doi.org/10.1155/2023/4034241

Research Article

Design and Development of Parasitic Elements Loaded Quadband Frequency and Pattern Reconfigurable Antenna

K. Karthika [1] **and K. Kavitha** [2]

[1]*Department of Electronics and Communication Engineering, Kumaraguru College of Technology, Coimbatore, India*
[2]*Department of Electronics and Communication Engineering, Velammal College of Engineering and Technology, Madurai, India*

Correspondence should be addressed to K. Karthika; karthika.svk@gmail.com

Received 23 March 2023; Revised 2 May 2023; Accepted 9 May 2023; Published 23 May 2023

Academic Editor: Xiao Ding

Modern communication demands a low-profile, versatile antenna. In this paper, a low-profile antenna of size $38 \times 40 \times 0.787$ mm^3 is proposed to reconfigure frequency and radiation pattern. The Rogers RT Duroid 5870 of dielectric constant 2.33 is used as a substrate. Frequency reconfiguration is achieved by connecting patches of different lengths corresponding to the resonant frequencies through three PIN diode switches. Switching on/off these three diodes results in frequency switching between four distinct frequency bands. The Yagi-Uda principle is utilized to alter the radiation pattern. Simple parasitic elements are loaded on either side of the radiating structure. Changing the electrical lengths of the parasitic elements using PIN diode switches facilitates pattern reconfiguration by making them behave as a reflector/director. The presented structure resonates at four distinct frequencies (5.3 GHz/3.82 GHz/2.77 GHz/2.2 GHz) with a maximum of three beam tilt angles for each resonating frequency. SMP1345-079LF PIN diode is used for switching operation. Biasing circuit has been designed to ensure RF and DC isolation. The proposed antenna offers acceptable radiation performance in all the switching states. The average measured gains are 2.43 dBi, 2.42 dBi, 3.5 dBi, and 3.29 dBi at 5.3 GHz, 3.82 GHz, 2.77 GHz, and 2.2 GHz, respectively. On an average, the proposed antenna exhibits the simulated efficiency of 81%. The proposed antenna is suitable for 5G communication as its bandwidth covers band 1, band 7, band 46, and band 77 of the 5G new radio (NR) standard. Fabrication and testing are done to validate the results.

1. Introduction

The integration of several applications into one device is necessary for contemporary wireless communication systems. To accomplish this, the system can either employ a single antenna with many functionalities or incorporate multiple antennas inside the device. The use of several antennas in a single system to support multiple applications is not a viable solution. Multiple antennas in a single system require more area to deploy, interfere with one another, have more installation costs, and have more complicated hardware platforms. Reconfigurable antennas are one of the potential methods for addressing the above-stated requirements [1]. The need for reconfigurable antennas is further driven by the demand for wireless communication systems that require antennas to adapt to changing operational conditions. Reconfigurable antennas can provide frequency agility, beam steering, polarization control, multimode operation, and miniaturization, making them a critical component of modern wireless communication systems. Reconfiguration can be achieved through electrical switches/mechanical switches/optical switches/reconfigurable materials/structural alterations [2]. The majority of research on reconfigurable antennas concentrated on a single reconfiguration like either frequency or pattern or polarization.

Reconfigurable antennas can be designed to operate over a range of frequencies, allowing them to adapt to changing frequency bands in wireless communication systems. This can be particularly important in situations where frequency allocation is limited or when sharing of frequency bands is required. Spectrum can be effectively used with frequency reconfigurable antennas. A compact antenna that can switch frequencies

among thirty-six different states with a stable radiation pattern is presented in [3]. Six-pin diodes are loaded along the non-radiating edges of the patch. By connecting the ground plane and non-radiating edges of the patch with PIN diodes, the operating frequency can be altered. In [4], two PIN diodes are positioned in the feed line to switch between the wideband and triband modes of operation. [5] suggests an E-shaped antenna design reconfigure between six operating frequencies. The transmission line model theory is applied to compute the antenna's effective length. Two PIN diodes are employed to achieve frequency reconfiguration. Conformal antennas may be a preferable option for many practical applications. The conformal antenna's relevance in modern applications is enhanced by including reconfigurability. A flexible CPW-fed frequency agile antenna has been proposed in [6]. Switching on/off the PIN diode located in its structure changes its resonant length and offers reconfiguration between five distinct frequencies.

Pattern reconfiguration allows the antenna to direct the radiation pattern towards a specific location or direction. This can be particularly important in situations where there are multiple signal sources or when the antenna needs to track a moving target. By changing the radiation pattern, the antenna can avoid or reduce the interference caused by unwanted signal sources. Antennas loaded with parasitic elements follow the Yagi-Uda principle to realize pattern reconfiguration [7–10]. Four folded monopoles are positioned along the $+X$, $-X$, $+Y$, and $-Y$ directions, respectively. Then, the monopoles are connected to the main radiator positioned in the center via PIN diode switches. When any of the folded monopoles is connected to the main antenna, it behaves as a director, and the remaining three behave as a reflector. Using this way, the radiation pattern is deflected in four different directions [8]. Stubs loaded on the ground plane performs as a reflector or director to alter the radiation pattern par with the switching state [9]. In [11], pattern reconfiguration is accomplished by placing the switchable parasitic strip between the reflector and the monopole antenna. Pattern reconfiguration can also be accomplished through single to multiple excitations in an antenna design [12]. The radiation pattern can be continuously steered in different directions by mechanically rotating a semicircular metasurface disk over the circular patch antenna [13].

Incorporating hybrid reconfiguration capability in a single radiating structure satisfies the need for a contemporary communication system. Pattern and frequency reconfigurable antennas have a wide range of applications in wireless communication systems, radar systems, military and defense, medical imaging, and IoT applications. These antennas can provide better signal quality, coverage, and imaging resolution and adapt to changing operational conditions. In recent years, notable works have contributed towards compound reconfiguration like a combination of frequency, polarization, and pattern reconfiguration. Incorporation of pattern agility in frequency reconfigurable antennas improves the performance of wireless systems by reducing source noise, enhancing security, and conserving energy by directing the signal in the intended direction [14]. In 5G networks, there is a growing demand for pattern and frequency reconfigurable antennas (PFRA). These antennas can provide directional radiation patterns that can be dynamically adjusted to suit the changing requirements of the network. Further, it can be designed to operate on multiple frequency bands, allowing them to switch between different frequency bands to avoid interference. Overall, designing a compact, highly efficient PFRA can offer a significant advantage in 5G networks by providing the flexibility, adaptability, and efficiency required to support the diverse range of applications and services that will be enabled by this technology. Several frequencies and pattern reconfigurable antennas are discussed in the literature. Most reconfigurable antennas use a rectangular patch as their basic structure. The impact of biasing lines in resonating frequency is inhibited by positioning them away from the antenna [15]. Four PIN diodes positioned along the two horizontal slits of a rectangular patch perform frequency reconfiguration and pattern reconfiguration [16].

The work presented in [17] utilizes four metallic strips of different lengths and four PIN diodes to perform pattern and frequency reconfiguration. Wideband operation in such antennas can be achieved by utilizing a symmetrical structure [18]. In [19], a modified rectangular patch with a single PIN diode is reported to perform frequency reconfiguration. Here, the stubs loaded on either side of the ground plane change the ground current and steer the beam direction based on the switching states. Parasitic patches and twelve PIN diodes are utilized to reconfigure the pattern and frequency presented in [20]. To perform pattern reconfiguration, a planar Yagi-Uda antenna on a coplanar structure is proposed in [21]. Two parasitic strips along with switches are loaded on the back side of the designed coplanar structure. Depending on the switching states, these parasitic strips either function as a reflector or a director. However, the majority of the reported compound reconfigurable antennas have relatively large sizes and utilize a greater number of actuators, complex biasing circuitry design, and limited operating bands.

Sub-6 GHz frequencies, which are typically in the frequency range between 600 MHz and 6 GHz, are used in 5G applications to provide large area coverage and high data rates. Band 1 (2.11-2.17 GHz), band 7 (2.62-2.69 GHz), band 46 (5.15-5.925 GHz), and band 77 (3.3-4.2 GHz) are some of the most widely used 5G new radio (NR) frequency bands. The proposed work is inspired and motivated by research challenges in the 5G network. This work focuses on the creation of a compact compound-reconfigurable antenna operating in the above-listed bands of 5G application. The following are the major contributions of this proposed work.

(i) Design of a low-profile novel structure to reconfigure frequency and radiation pattern

(ii) Design of biasing circuit to ensure RF and DC isolation

(iii) Implementation of frequency reconfiguration by connecting patches of different lengths through PIN diode switches

(iv) Pattern modification using the Yagi-Uda principle is available in the literature. In most of the works,

the pattern is changed by loading inverted L-shaped parasitic strips or dumbbell-shaped parasitic strips to the other side of the radiating element. In this work, simple parasitic strips are positioned along the radiating elements, and fewer diodes are utilized to realize pattern reconfiguration without altering the resonant frequency

The design evolution of the proposed antenna is presented in Section 2 of this research article. The findings of the simulation, measurement, and the proposed work's comparison with the existing state-of-the-art in literature are discussed in Section 3. The proposed work is concluded in Section 4.

2. Antenna Design

The proposed compound reconfigurable antenna printed on a substrate Rogers RT Duroid of dielectric constant 2.33 and thickness of 0.787 mm is depicted in Figure 1. The overall size of the presented microstrip-fed structure is $38 \times 40 \times 0.787\ \text{mm}^3$. The effective resonant lengths (L_{f_r}) of the radiating elements are calculated using (1) and (2) [22].

$$L_{f_r} = \frac{c}{4f_r\sqrt{\varepsilon_{\text{eff}}}}, \tag{1}$$

$$\varepsilon_{\text{eff}} = \frac{\varepsilon_r + 1}{2} + \frac{\varepsilon_r - 1}{2}\left(1 + 12\left(\frac{w}{h}\right)\right)^{-0.5}, \tag{2}$$

where ε_{eff} denotes an effective dielectric constant, f_r represents resonating frequency, c indicates free space velocity, ε_r denotes the dielectric constant, and w and h indicate the width and thickness of the trace and the substrate, respectively.

For frequency reconfiguration, three radiating patches of different resonant lengths are designed and linked to the main radiator (P_1) through three PIN diode switches (D1, D2, and D3). Pattern reconfiguration is accomplished based on the Yagi-Uda principle. Parasitic elements are loaded on either side of the radiating elements. PIN diodes D4 and D5 are loaded along the respective parasitic elements to perform pattern reconfiguration. The proposed compound reconfigurable antenna's design evolution is shown in Figure 2.

2.1. Frequency Reconfiguration. The first step in the proposed structure's evolution is the design of the main radiator. The main radiator resonating at 5.2 GHz is achieved by modifying its effective resonant length through structural alteration. The calculated effective resonant length of the main radiating element (P_1) is optimized to 5.6 mm. Further, the partial ground plane's length (Lg) is varied and analyzed through parametric analysis as depicted in Figure 3. At Lg = 8.2 mm, good impedance matching is observed for 5.2 GHz. The effective resonant length to have resonance at 3.8 GHz is calculated and optimized to 10.4 mm by connecting a patch (P_2) of length 3.1 mm to the main radiator (P_1) via PIN diode switch D1 (ON) (step 2 of Figure 2).

To provide proper biasing of the PIN diode, two RF choke inductors (to block the RF signal and pass the DC signal) and a DC block capacitor (to prevent the DC signal

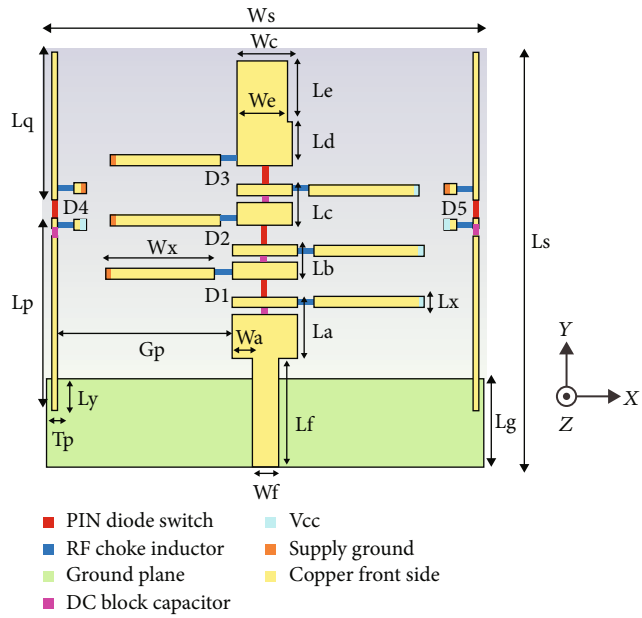

Figure 1: Proposed compound reconfigurable antenna - geometry (parameters: Ls = 38 mm, Ws = 40 mm, Lg = 8.2 mm, Lf = 10 mm, Wf = 2.356 mm, La = 5.6 mm, Lb = 3.1 mm, Lc = 3.85 mm, Ld = 4 mm, Le = 5.5 mm, Wa = 2 mm, Wc = 5 mm, We = 4.5 mm, Lp = 16.6 mm, Lq = 13.5 mm, Tp = 0.5 mm, Lx = 1 mm, Wx = 10 mm, Gp = 16 mm, Ly = 2 mm, h = 0.787 mm).

from interfering with the RF signal) are utilized. A slit has been made in the main radiator, and the capacitor is positioned along the slit rather than being given a separate space. To connect the RF choke inductors to the power supply, DC biasing lines/DC biasing patches have been designed and placed close to the radiating element as shown in step 3 of Figure 2. The dimensions of the DC biasing patch are chosen such that the performance of the antenna is not disrupted. Moreover, Figure 4 projects that the inclusion of biasing circuit for D1 does not have a significant impact on the proposed antenna's performance.

Switching on/off the diode D1 switches its operating frequency between 5.2 GHz and 3.8 GHz. In step 4, a patch (P_3) of a length of 3.85 mm is connected to the P_2 through D2. Switching on the diodes D1 and D2 increases the effective resonant length to 15.95 mm resulting in resonance at 2.9 GHz. To further achieve resonance at 2.1 GHz, a patch (P_4) of length 9.5 mm is connected to P_3 via D3 (on) (step 6 of Figure 2). However, the design offers dual resonance at 2.47 and 5.69 GHz. Hence, the shape of P_4 is modified to achieve the desired single resonance. Modified P_4 structure (step 7 of Figure 2) offers return loss below -10 dB at 2.17 GHz. The required biasing for D2 and D3 has been included, as specified in step 3, and it is shown in steps 5 and 8 of Figure 2.

2.2. Pattern Reconfiguration. The final step in the proposed design is aimed at pattern reconfiguration. Parasitic elements can be used for pattern reconfiguration by adjusting the length, distance, and orientation of the parasitic element relative to the main antenna element. This will change the phase and amplitude of the signal at different points in the

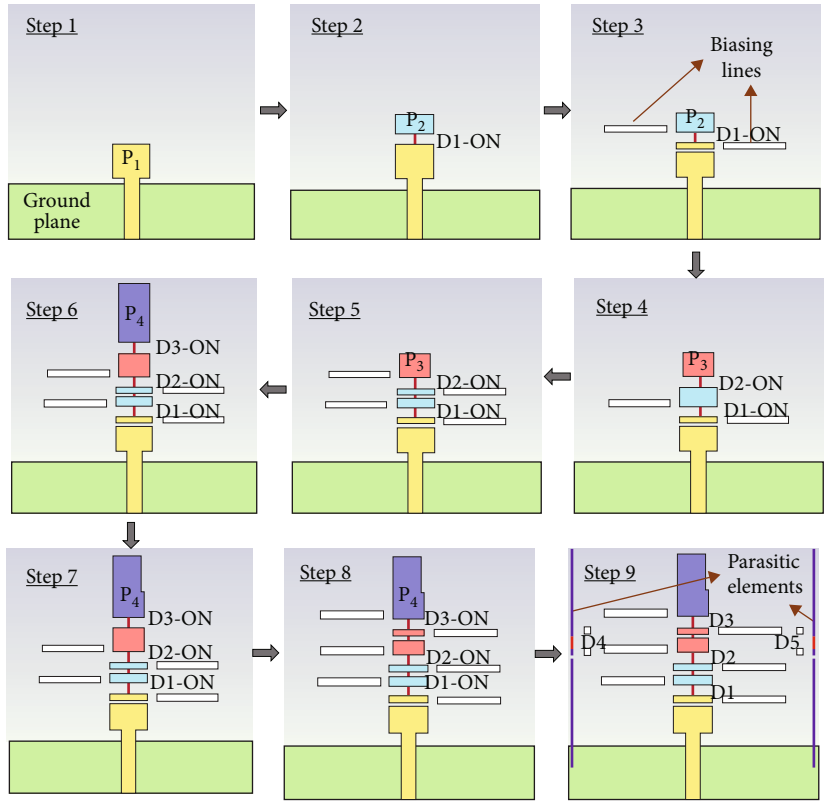

FIGURE 2: Proposed structure—design evolution.

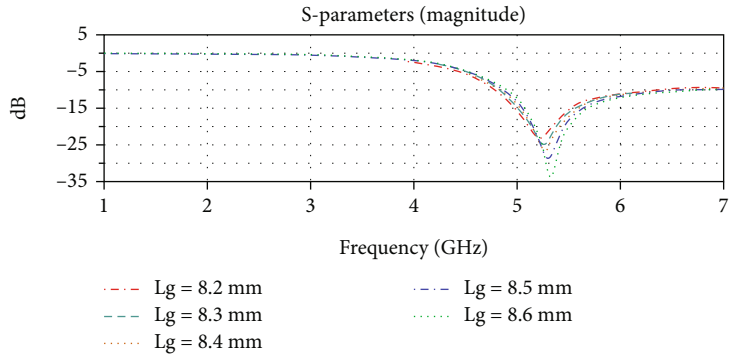

FIGURE 3: Parametric analysis—length of the ground plane (Lg).

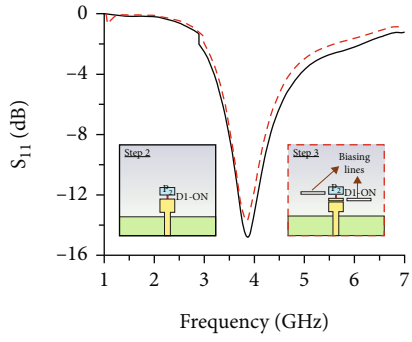

FIGURE 4: Design evolution—return loss plot: step 2 (without biasing circuit) and step 3 (with the biasing circuit).

antenna, which will in turn change the radiation pattern. Two parallel parasitic elements of width 0.5 mm and length 31.8 mm are loaded to the sides of the designed antenna. These elements act as a reflector/director, and two PIN diode switches (D4 and D5) are positioned along the length of the two parasitic elements to facilitate pattern reconfiguration. Henceforth, the proposed structure can reconfigure frequency and pattern as well.

The radiation property is significantly impacted by the coupling length (Ly) between the parasitic element and the ground plane. The coupling length and the distance between the main radiator and parasitic elements (Gp) are obtained by performing a parametric sweep. Figures 5 and 6 present the parametric analysis of Ly and Gp, respectively. The

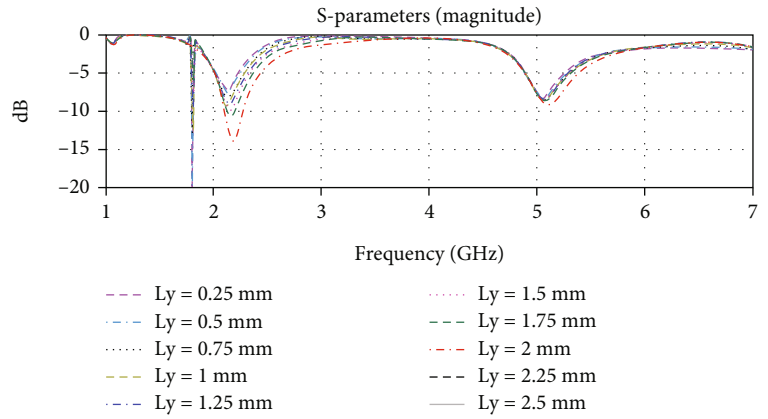

Figure 5: Parametric analysis of Ly.

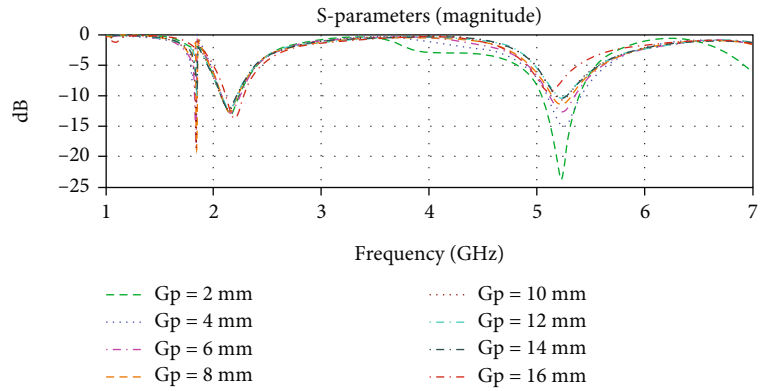

Figure 6: Parametric analysis—effect of varying the distance between the radiator and parasitic elements (Gp).

designed antenna is analyzed for Ly = 0.25 mm to 2.5 mm and Gp = 2 mm to 16 mm in case I-S4. The simulation reveals that the additional resonance is observed at 1.8 GHz in the simulated range excluding the value of Ly = 2 mm. At Ly = 2 mm, the additional resonance is nullified, and the resonance is observed at the intended resonating frequency of 2.17 GHz. At Gp = 16 mm, only the intended resonance is observed. Hence, the coupling length and the space between the radiating and parasitic elements are finalized as 2 mm and 16 mm, respectively.

To perform the switching operation, the SMP1345-079 LF PIN diode is used. It offers high-speed switching and is suitable for switch applications from 10 MHz to 6 GHz. The on state equivalent circuit of this diode is achieved by connecting $R = 1.5\,\Omega$ in series with $L = 0.7$ nH. The off state equivalent circuit of this diode is achieved by connecting the parallel combination of $R = 1000\,\Omega$ and $C = 0.18$ pF in series with $L = 0.7$ nH. Since the design involves PIN diodes for switching operation, a biasing circuit has been designed for proper excitation of the switches. The space for placement of PIN diode switches, capacitors, and inductors is decided as per data sheets.

3. Results and Discussion

The proposed antenna is analyzed for three cases. In case I, both D4 and D5 are in the OFF state. D4 is off and D5 is on for case II. D4 is on, and D5 is off in case III. Each of the cases is analyzed for four switching states: switching state 1 (S1)—(D1-off, D2-off, and D3-off), switching state 2 (S2)—(D1-on, D2-off, and D3-off), switching state 3 (S3)—(D1-on, D2-on, and D3-off), and switching state 4 (S4)—(D1-on, D2-on, and D3-on). Frequency and pattern reconfigurability are observed through the comparative analysis of case II and case III concerning case I.

3.1. Case I: Frequency Reconfigurability Mode. In case I, the switching state 1 exhibits resonance at 5.2 GHz (4.71-5.84 GHz). Switching on D1 (case I-S2) connects P_1 and P_2 . This lengthens the current distribution and shifts the resonating frequency to 3.8 GHz (3.44-4.17 GHz). Case I-S3 mode increases the length further by turning ON D2. In this mode, the proposed antenna resonates at 2.9 GHz (2.61-3.13 GHz). In case I-S4 mode, resonance is observed at 2.17 GHz (2.08-2.27 GHz).

3.2. Cases II and III: Frequency and Pattern Reconfigurability Mode. Frequency and pattern reconfigurability are seen in cases II and III. The switching states S1, S2, S3, and S4 are analyzed for the abovementioned cases. The observed resonant frequencies for case II and case III's S1 are like the case I-S1 (5.2 GHz). In case I-S1, the main beam direction in the x-z plane is along -97^0. Now, in case II-S1, switching off D4 makes the left parasitic element ($-x$ direction) behave as a

director, and switching on D5 makes the right parasitic element (+x direction) behave as a reflector. As a result, the main lobe direction is changed to -164^0 (−x direction). Whereas in case III-S1, switching on and off the D4 and D5 makes the left parasitic element (−x direction) function as a reflector and the right parasitic element (+x direction) as a director, respectively. This shifts the main lobe direction to +164^0 (+x direction). Hence, the radiation pattern of the designed antenna is reconfigurable.

Similarly, frequency and pattern reconfiguration are observed for all the remaining switching states of case II and case III. In case II, the main lobe direction in the x-z plane (phi = 0^0) is -90^0 at 3.8 GHz, -100^0 at 2.9 GHz, and 2.17 GHz. Whereas +90^0, +100^0, and +100^0 are observed for case III at 3.8 GHz, 2.9 GHz, and 2.17 GHz, respectively. This implies that the switching state of D4 and D5 switches the radiation pattern without altering the resonating frequencies of the radiating structure.

The proposed antenna is fabricated, and its measurement setup is depicted in Figure 7. The front and back views of the fabricated antenna are shown in Figures 7(a) and 7(b). The vector network analyzer (VNA) measurement setup for return loss measurement is seen in Figure 7(c). It is noted that the biasing lines are connected to the power supply for switching on/off the PIN diodes. Gain and pattern measurements are done using anechoic chamber measurement as depicted in Figure 7(d).

The measured results of all three cases are summarized in Figure 8 and are discussed as follows. Figure 9(a) presents an S_{11} comparison of the simulated and measured results for case I, whereas Figure 9(b) projects an S_{11} comparison of the simulated and measured results for case II and case III. Depending on the states of D1-D3, the design reconfigures to 5.3 GHz, 3.82 GHz, 2.77 GHz, and 2.2 GHz. When comparing the measured results with the simulation findings, slight variations in the resonant frequencies are observed due to the presence of biasing wires in the measurement setup. In case I, the bandwidths obtained at 5.3 GHz, 3.82 GHz, 2.77 GHz, and 2.2 GHz are 1225 MHz (5-6.225 GHz), 300 MHz (3.67–3.97 GHz), 900 MHz (2.625–3.525 GHz), and 335 MHz (2.09–2.425 GHz), respectively. In both case II and case III, 850 MHz (5-5.85 GHz), 425 MHz (3.675–4.1 GHz), 545 MHz (2.625–3.17 GHz), and 321 MHz (2.09–2.411 GHz) are the bandwidths obtained at 5.3 GHz, 3.82 GHz, 2.77 GHz, and 2.2 GHz, respectively. Figure 9(c) projects the average gain and efficiency of the proposed antenna. The average measured gain of 2.43 dBi, 2.42 dBi, 3.5 dBi, and 3.29 dBi is observed at 5.3 GHz, 3.82 GHz, 2.77 GHz, and 2.2 GHz, respectively. On average, a radiation efficiency of around 81% is obtained for the simulated antenna design. Further, the functionality of the proposed design is analyzed w.r.t their radiation pattern and surface current distribution.

xIn Figure 10, the simulated radiation pattern (black dotted line) in the x-z plane (phi = 0^0) is compared with the measured radiation pattern (red solid line). The red solid arrow mark in all the switching cases indicates the main lobe's direction. The patterns in Figure 10 are used to identify the directionality and the direction of the main lobe under different switching conditions. Changing the states of D4 and D5 reconfigures the radiation pattern from bidirectional to unidirectional at 5.3 GHz and omnidirectional to unidirectional at 3.82 GHz, 2.77 GHz, and 2.2 GHz. In case I-S1, the direction of the main lobe is -97^0. It is tilted to -165^0 and +165^0 in case II-S1 and case III-S1, respectively. Henceforth, at 5.3 GHz, the beam steering angles are –68^0 and +262^0. In case I-S2, the main lobe direction is +115^0. This direction is changed to -93^0 and +93^0 in case II-S2 and case III-S2, respectively. The observed beam steering angles at 3.82 GHz are +152^0 and –22^0.

The main lobe oriented towards +180^0 in case I-S3 has been shifted to -105^0 in case II-S3 and +105^0 in case III of S3. Hence, the beam steering angles of ±75^0 are obtained at 2.77 GHz. The same has been observed for switching state 4, and the corresponding beam steering angles at 2.2 GHz are ±75^0. In frequency and pattern reconfiguration, reconfiguring the frequency should not affect the radiation pattern and vice versa. It is observed that the beam steering angles at 2.77 GHz and 2.2 GHz remain the same. However, it differs at 5.3 GHz and 3.82 GHz. The presence of bias lines will have an impact on the antenna's radiation pattern. This will occur due to the coupling between bias lines and the radiating elements. To minimize this impact, the placement and orientation of bias lines are done carefully within the antenna structure. However, distortion in the pattern reduced realized gain, and shift in the resonant frequencies is seen in the measured results. Creating vias in the required biasing positions will make the bias lines move to the other side of the radiating elements. This technique can be used in future work to lessen the effects of bias lines.

Figure 11 illustrates the surface current distribution. According to the switching condition, a high surface current distribution is seen at the radiating structures. It is observed that the high current distribution in the main radiator and the feed line for all three cases in switching state 1 offers resonance at 5.2 GHz. In addition to that, during all the three cases, a high current density noted in the P_2 (during switching state 2),P_3 (during switching state 3), and P_4 (during switching state 4) contributed to resonance at 3.8 GHz, 2.9 GHz, and 2.17 GHz, respectively. Further, for all the switching states in case I, the current density is minimal in the parasitic elements.

The surface current on the reflector may be relatively low compared to other elements in the antenna. This is because the reflector's primary function is to reflect and redirect energy from the radiating element, rather than directly radiating energy itself. The director in the antenna is used to focus the energy on a particular direction. Hence, the surface current on the directors is typically higher than the surface current on the reflector or driven element. In case II, the high surface current is noted along the left parasitic element, and the low surface current is observed along the right parasitic element for all the switching states. Hence, the left parasitic element acts as a director and the right parasitic element acts as a reflector in all the switching states of case II, whereas the vice versa is observed for all the switching states in case III.

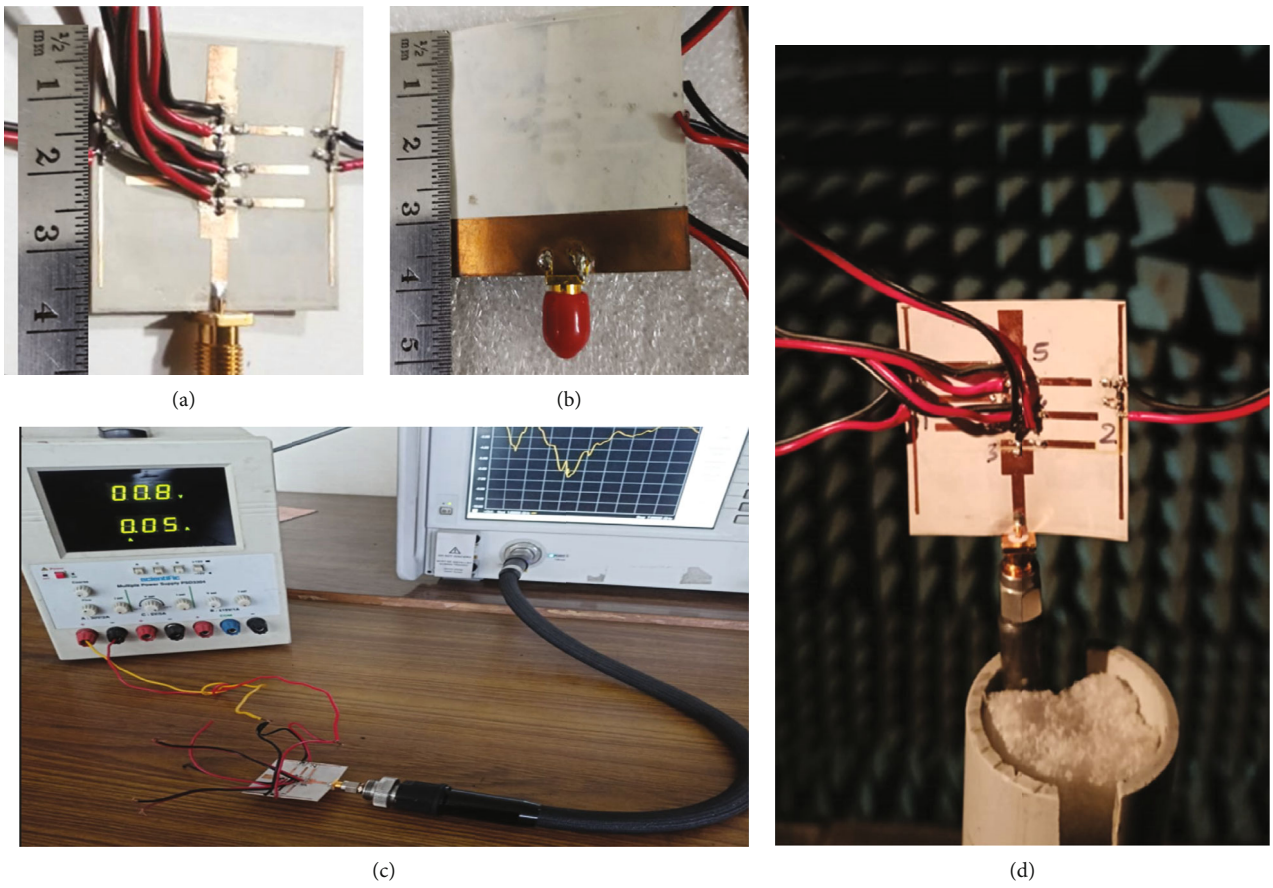

FIGURE 7: Measurement setup of fabricated antenna. (a) Top view, (b) rear view, (c) VNA testing, and (d) anechoic chamber measurement.

	Switching condition					Frequency (GHz)	S_{11} (dB)	Gain (dBi)	Bandwidth (MHz)	Main Lobe Direction (phi = 0^0)	Beam Steering Angle
	D1	D2	D3	D4	D5						
Case I - S1	OFF	OFF	OFF	OFF	OFF	5.3	−15.56	2.24	1225	-97^0	0^0
Case I - S2	ON	OFF	OFF	OFF	OFF	3.82	−12.18	2.38	300	$+115^0$	0^0
Case I - S3	ON	ON	OFF	OFF	OFF	2.77	−19.38	3.72	900	$+180^0$	0^0
Case I - S4	ON	ON	ON	OFF	OFF	2.2	−12.11	3.19	335	$+180^0$	0^0
Case II - S1	OFF	OFF	OFF	OFF	ON	5.3	−15.8	2.58	850	-165^0	-68^0
Case III - S1	OFF	OFF	OFF	ON	OFF		−15.8	2.48	850	$+165^0$	$+262^0$
Case II - S2	ON	OFF	OFF	OFF	ON	3.82	−13.22	2.45	425	-93^0	$+152^0$
Case III - S2	ON	OFF	OFF	ON	OFF		−13.21	2.42	425	$+93^0$	-22^0
Case II - S3	ON	ON	OFF	OFF	ON	2.77	−19.09	3.35	545	-105^0	$+75^0$
Case III - S3	ON	ON	OFF	ON	OFF		−19.07	3.33	545	$+105^0$	-75^0
Case II - S4	ON	ON	ON	OFF	ON	2.2	−12.09	3.34	321	-105^0	$+75^0$
Case III - S4	ON	ON	ON	ON	OFF		−12.12	3.35	321	$+105^0$	-75^0

Switching conditions responsible for only frequency reconfiguration
Switching conditions responsible for only pattern reconfiguration

FIGURE 8: Measured results of proposed compound reconfigurable antenna.

The performance comparison summarized in Table 1 reveals that the presented work offers a low-profile, compact structure on comparing with [1, 16, 18, 20, 23, 24, 26–28]. The presented work requires fewer switches than [25, 28]. Using five switches, the suggested work operates at more operating bands than [1, 29]. This work has reduced design complexity by eliminating the separate layer for the biasing circuit as in [19, 20, 22].

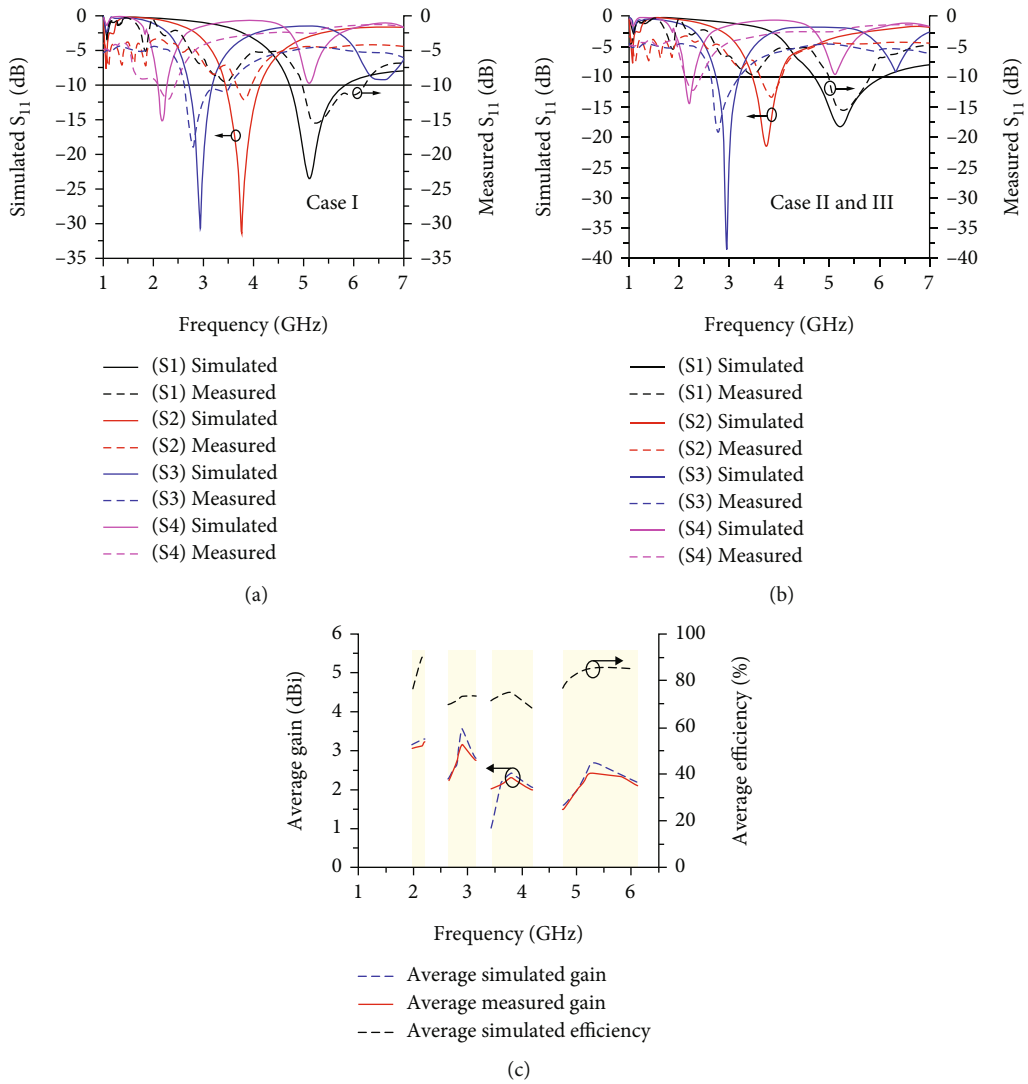

Figure 9: Results: (a) case I—return loss, (b) cases II and III—return loss, and (c) gain and efficiency.

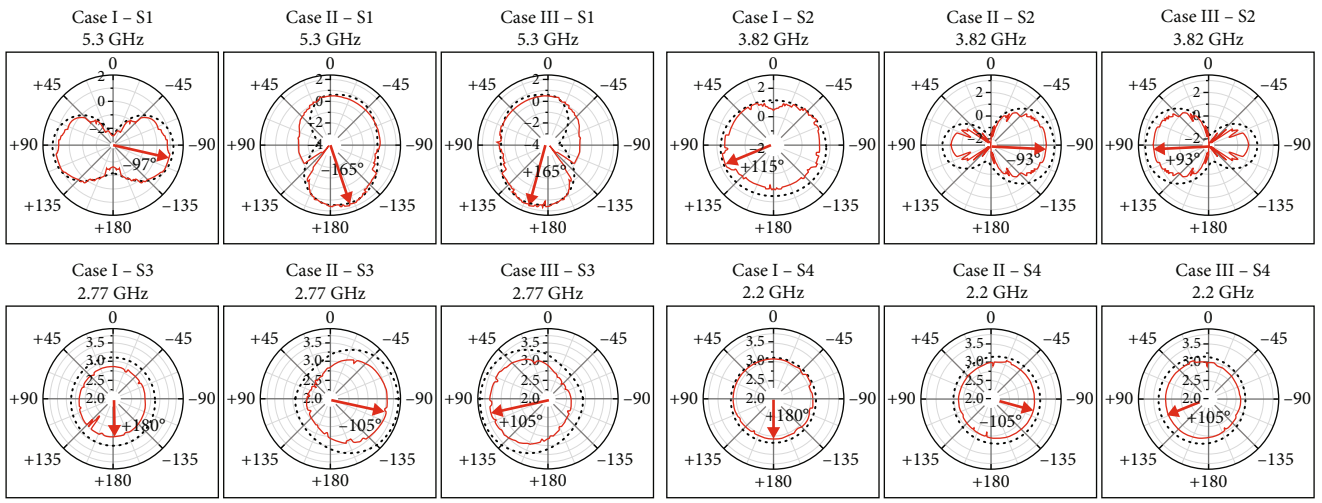

Figure 10: Radiation pattern (phi = 0^0) (*x*-*z* plane) (simulated result—black dotted line, measured result-red solid line).

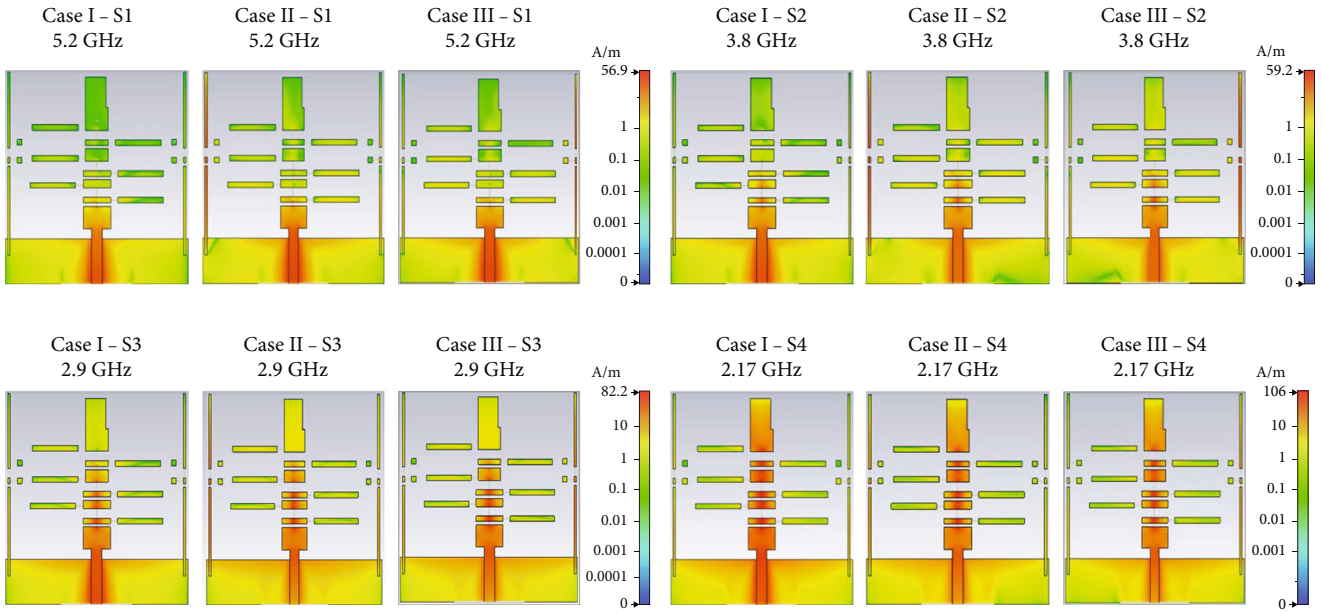

Figure 11: Simulated result—surface current distribution.

Table 1: Proposed work vs. existing frequency and pattern reconfigurable antennas.

Ref. no.	Dimension ($L \times W \times h$) (mm^3)	No. of switches/means of switching	Maximum number of beams	No. of frequency bands	Peak gain (dBi)
[1]	$47 \times 80 \times 1.5$	5/PIN	2	2	2.7/2.6
[16]	$50 \times 50 \times 1.6$	4/PIN	3	4	4/3.8/4.4/5
[18]	$40 \times 30 \times 1.6$	4/PIN	3	2	2.45/2.76
[20]	$46 \times 32 \times 1.6$	12/PIN	5	5	1.25/2.80/2.90/3.64/4.67
[23]	70×70	4/PIN	3	2	6.214/8.461
[24]	$50 \times 100 \times 1.6$	2/PIN	2	2	4.9/5.5
[25]	$42 \times 44 \times 0.127$	8/PIN	2	2	—
[26]	$66.4 \times 66.4 \times 1.5$	3/RF MEMS	2	4	—
[27]	$120 \times 120 \times 7.362$	-/PIN	3	2	8-9 dB/6-10.31 dB
[28]	$112 \times 52 \times 0.508$	18/NMOS transistors	8	2	3.8/8.3
[29]	—	8/PIN	4	2	5.63/5.55
This work	$38 \times 40 \times 0.787$	5/PIN	3	4	2.43/2.42/3.5/3.29

4. Conclusion

A compact antenna that can reconfigure quadband and radiation pattern is reported in this article. The proposed antenna can reconfigure to 5.3 GHz, 3.82 GHz, 2.77 GHz, and 2.2 GHz. At each operating frequency, the antenna can steer its main lobe into three different directions. In all the resonating frequencies, acceptable gains are realized. The presented design reduces structural complexity by utilizing fewer diodes and simple biasing circuits. The antenna performs well with an average efficiency of 85%, 75%, 73%, and 91% at 5.3 GHz, 3.82 GHz, 2.77 GHz, and 2.2 GHz, respectively. The proposed antenna covers band 1, band 7, band 46, and band 77 of the 5G new radio (NR) standard. These bands are some of the most widely used 5G NR frequency bands. Hence, the proposed antenna is suitable for 5G applications in the sub-6 GHz frequency range.

Data Availability

The data used to support the findings of this study are included within the article.

Conflicts of Interest

The authors declare that they have no conflicts of interest.

Authors' Contributions

K. Karthika and K. Kavitha contributed to the conceptualization, methodology, results, and discussion.

References

[1] P. K. Li, Z. H. Shao, Q. Wang, and Y. J. Cheng, "Frequency- and pattern-reconfigurable antenna for multistandard wireless applications," *IEEE Antennas and Wireless Propagation Letters*, vol. 14, pp. 333–336, 2015.

[2] K. Karthika and K. Kavitha, "Reconfigurable antennas for advanced wireless communications: a review," *Wireless Personal Communications*, vol. 120, no. 4, pp. 2711–2771, 2021.

[3] A. Boukarkar, X. Q. Lin, Y. Jiang, and X. F. Yang, "A compact frequency-reconfigurable 36-states patch antenna for wireless applications," *IEEE Antennas and Wireless Propagation Letters*, vol. 17, no. 7, pp. 1349–1353, 2018.

[4] S. Sharma and C. C. Tripathi, "Wideband to concurrent triband frequency reconfigurable microstrip patch antenna for wireless communication," *International Journal of Microwave and Wireless Technologies*, vol. 9, no. 4, pp. 915–922, 2017.

[5] S. Ullah, S. Ahmad, B. A. Khan, U. Ali, F. A. Tahir, and S. Bashir, "Design and analysis of a hexa-band frequency reconfigurable monopole antenna," *IETE Journal of Research*, vol. 64, no. 1, pp. 59–66, 2018.

[6] A. Ahmad, F. Arshad, S. I. Naqvi, Y. Amin, H. Tenhunen, and J. Loo, "Flexible and compact spiral-shaped frequency reconfigurable antenna for wireless applications," *IETE Journal of Research*, vol. 66, no. 1, pp. 22–29, 2020.

[7] Z. Shi, R. Zheng, J. Ding, and C. Guo, "A novel pattern-reconfigurable antenna using switched printed elements," *IEEE Antennas and Wireless Propagation Letters*, vol. 11, pp. 1100–1103, 2012.

[8] G. Jin, M. Li, D. Liu, and G. Zeng, "A simple four-beam reconfigurable antenna based on monopole," *IEEE Access*, vol. 6, pp. 30309–30316, 2018.

[9] T. Aboufoul, S. Member, C. Parini, X. Chen, S. Member, and A. Alomainy, "Pattern-reconfigurable planar circular ultra-wideband monopole antenna," *IEEE Transactions on Antennas and Propagation*, vol. 61, no. 10, pp. 4973–4980, 2013.

[10] M. Jusoh, T. Aboufoul, T. Sabapathy, A. Alomainy, and M. R. Kamarudin, "Pattern-reconfigurable microstrip patch antenna with multidirectional beam for WiMAX application," *IEEE Antennas and Wireless Propagation Letters*, vol. 13, pp. 860–863, 2014.

[11] Y. Juan, W. Che, W. Yang, and Z. N. Chen, "Compact pattern-reconfigurable monopole antenna using parasitic strips," *IEEE Antennas and Wireless Propagation Letters*, vol. 16, pp. 557–560, 2017.

[12] B. Ashvanth, B. Partibane, M. G. N. Alsath, and R. Kalidoss, "Gain enhanced multipattern reconfigurable antenna for vehicular communications," *International Journal of RF and Microwave Computer-Aided Engineering*, vol. 30, no. 6, 2020.

[13] M. S. Alam and A. Abbosh, "Planar pattern reconfigurable antenna with eight switchable beams for WiMax and WLAN applications," *IET Microwaves, Antennas and Propagation*, vol. 10, no. 10, pp. 1030–1035, 2016.

[14] H. A. Majid, M. K. A. Rahim, M. R. Hamid, and M. F. Ismail, "Frequency and pattern reconfigurable slot antenna," *IEEE Transactions on Antennas and Propagation*, vol. 62, no. 10, pp. 5339–5343, 2014.

[15] A. A. Palsokar and S. L. Lahudkar, "Frequency and pattern reconfigurable rectangular patch antenna using single PIN diode," *AEU-International Journal of Electronics and Communications*, vol. 125, article 153370, 2020.

[16] Y. P. Selvam, M. Kanagasabai, M. G. N. Alsath et al., "A low-profile frequency- and pattern-reconfigurable antenna," *IEEE Antennas and Wireless Propagation Letters*, vol. 16, pp. 3047–3050, 2017.

[17] P. Thanki and F. Raval, "Fork-shaped frequency and pattern reconfigurable antenna," *International Journal of Communication Systems*, vol. 33, no. 17, article e4613, 2020.

[18] L. Han, C. Wang, W. Zhang, R. Ma, and Q. Zeng, "Design of frequency- and pattern-reconfigurable wideband slot antenna," *International Journal of Antennas and Propagation*, vol. 2018, Article ID 3678018, 7 pages, 2018.

[19] A. Iqbal, A. Smida, N. Mallat et al., "Frequency and pattern reconfigurable antenna for emerging wireless communication systems," *Electronics*, vol. 8, no. 4, p. 407, 2019.

[20] I. Ahmad, W. U. R. Khan, H. Dildar et al., "A pentaband compound reconfigurable antenna for 5G and multi-standard sub-6GHz wireless applications," *Electronics*, vol. 10, no. 20, p. 2526, 2021.

[21] S. Raman, N. Timmons, and J. Morrison, "Gain enhanced pattern reconfigurable planar Yagi-Uda antenna on coplanar structure," *Electronics Letters*, vol. 49, no. 25, pp. 1593–1595, 2013.

[22] I. Ahmad, H. Dildar, W. U. R. Khan et al., "Design and experimental analysis of multiband compound reconfigurable 5G antenna for Sub-6 GHz wireless applications," *Wireless Communications and Mobile Computing*, vol. 2021, Article ID 5588105, 14 pages, 2021.

[23] R. Dewan, M. K. A. Rahim, M. R. Hamid, M. Himdi, H. A. Majid, and N. A. Samsuri, "HIS-EBG unit cells for pattern and frequency reconfigurable dual band array antenna," *Progress in Electromagnetics Research*, vol. 76, pp. 123–132, 2018.

[24] M. S. Khan, A. Iftikhar, A. D. Capobianco, R. M. Shubair, and B. Ijaz, "Pattern and frequency reconfiguration of patch antenna using PIN diodes," *Microwave and Optical Technology Letters*, vol. 59, no. 9, pp. 2180–2185, 2017.

[25] Z. Zhu, P. Wang, S. You, and P. Gao, "A flexible frequency and pattern reconfigurable antenna for wireless systems," *Progress in Electromagnetics Research*, vol. 76, pp. 63–70, 2018.

[26] S. K. Patel, C. Argyropoulos, and Y. P. Kosta, "Pattern controlled and frequency tunable microstrip antenna loaded with multiple split ring resonators," *IET Microwaves, Antennas and Propagation*, vol. 12, no. 3, pp. 390–394, 2018.

[27] A. X. Chen and X. Liu, "The high gain frequency-and radiation pattern-reconfigurable antenna based on meta-surface," in *Progress in electromagnetics research symposium-Fall (PIERS-FALL)*, pp. 565–569, Singapore, 2017.

[28] M. K. Shereen, M. I. Khattak, and M. Al-Hasan, "A frequency and radiation pattern combo-reconfigurable novel antenna for 5G applications and beyond," *Electronics*, vol. 9, no. 9, p. 1372, 2020.

[29] K. Saurav, D. Sarkar, and K. V. Srivastava, "A dual-band reconfigurable Yagi–Uda antenna with diverse radiation patterns," *Applied Physics A: Materials Science & Processing*, vol. 123, no. 7, pp. 1–8, 2017.